



Phytoplankton morphological traits and biomass outline community dynamics in a coastal ecosystem (Gulf of Trieste, Adriatic Sea)

Ivano Vascotto^{1,2,3} · Patricija Mozetič³ · Janja Francé³

Received: 31 January 2024 / Accepted: 10 September 2024
© The Author(s) 2024

Abstract

Trait-based ecology has recently gained increasing importance in phytoplankton research. In particular, the taxonomic and morphological traits, such as size and shape of phytoplankton cells, can help to unveil the ecological processes and their drivers in the pelagic domain. Our study aims to shed light on the trophodynamics of phytoplankton communities in a coastal ecosystem in the northern Adriatic Sea (Gulf of Trieste) using data on individual traits such as biomass, size and shape of phytoplankton taxa during a one-year study. The phytoplankton parameters were investigated at the levels of the whole community, groups, and individual cells, analysing also the probability distributions of biomass and size of the latter level. The results showed good agreement between abundance and biomass data, as well as individual size and biomass with differences partly explained by cell shapes. We have emphasized the role of the local freshwater source in bottom-up control, alternating with top-down control of phytoplankton dynamics through taxonomic and morphological diversity. The predominant bimodal and non-power law distribution, especially during and around the biomass peaks, confirmed the importance of nano- and microphytoplankton size classes and the role of blooms in destabilizing the trophic webs. We suggest that the analyses of distribution types of individual cell size and biomass can be appropriate to spot ecological processes driving to unconstrained phytoplankton proliferation or to periods of trophic web stability.

Keywords Phytoplankton · Biomass · Size · Power law · Northern Adriatic

Introduction

Phytoplankton communities play an important role in marine ecosystems, as they are the gateway to pelagic food chains and are critical to biogeochemical cycling in the seas and oceans (Falkowski et al., 2003; Hays et al., 2005). The common characteristics used to describe phytoplankton communities and their dynamics are biomass, abundance, and taxonomic composition, with biomass, expressed as chlorophyll-a concentration, being largely used in ecological studies because it overwhelms all photoautotrophic microorganisms regardless of their size and

taxonomic affiliation. As such, chlorophyll-a biomass is a suitable indicator for assessing the ecological or trophic status of water bodies in the context of various environmental policies (e.g. European Directives 2000/60/ EC and 2008/56/ EC) (Varkitzi et al., 2018). On the other hand, biomass in the form of cellular carbon is used as a crucial parameter to define the phytoplankton component in the study of biogeochemical cycles or in ecosystem modelling (Aumont et al., 2015; Falkowski et al., 2003). Carbon biomass is usually calculated from cell biovolume through standard conversion factors (Menden-Deuer & Lessard, 2000; Socal et al., 2010), and biovolume in turn depends on cell size, which is therefore a very important measurable phytoplankton trait (Finkel et al., 2009). Indeed, according to the “metabolic theory” of Brown (2004), body size is one of the three key factors along with temperature and stoichiometry that influence individual’s metabolism and consequently community ecology. Body, i.e. cell size in phytoplankton, was recognized to offer potential advantages over standard taxonomic descriptors in community organization studies (Vadrucci et al., 2007),

✉ Ivano Vascotto
ivascotto@ogs.it

¹ Jozef Stefan International Postgraduate School, Jamova Cesta 39, 1000 Ljubljana, Slovenia

² National Institute of Oceanography and Applied Geophysics, Borgo Grotta Gigante, 42/C, 34010 Sgonico, TS, Italy

³ National Institute of Biology, Marine Biology Station Piran, Fornače 41, 6330 Piran, Slovenia

and is, along with the associated value of biovolume of critical importance in allometric studies (Beardall et al., 2009; Niklas, 2004; Verdy et al., 2009). In addition, cell size is among the functional traits that regulate competitive ability (e.g. nutrient uptake rates, growth rates) (Nock et al., 2016) and has as such a pivotal role in the field of trait based ecology of phytoplankton (Litchman & Klausmeier, 2008).

When coming to distributional properties, phytoplankton biomass is often assumed to follow the power law (Kostadinov et al., 2009, 2010; Kriest & Evans, 1999; Niklas, 2004), which has been shown to be correct on a global scale (Perkins et al., 2019). Under such an assumption, the biomass is uniformly distributed along log-scaled body size classes and its distribution describes a line in a log–log frequency biomass diagram (Sheldon et al., 1972). Since the literature on power law distribution of phytoplankton size uses the term “size” in the sense of “body size”, “biovolume” or “biomass” (Andersen et al., 2016; Finkel et al., 2009; Heneghan et al., 2019; Marquet et al., 2005), it is not clear whether the body size parameters of phytoplankton (for example length, diameter), also follow a power law. It has been suggested that the power law distribution can emerge from stable trophic networks (Bascompte, 2007; Newman, 2005) and that deviations from this distribution indicate the presence of ecological processes and human impacts operating at specific organism sizes and spatial scales (Armstrong, 1999; Cavender-Bares et al., 2001; Hatton et al., 2021). When biomass is assessed at the mesoscale, deviations from the power law are found in nearshore marine waters and in freshwater ecosystem (Sprules, 1988; Witek & Krajewska-Soltys, 1989). Such deviations have been associated with the seasonal blooms (Witek & Krajewska-Soltys, 1989) and with shifts from bottom-up to top-down control (Sprules, 1988). From these studies, it emerges that knowledge about cell size distribution provides valuable information not only about the phytoplankton community, but also about the state of its ecological relationships with other biological components (for example, zooplankton).

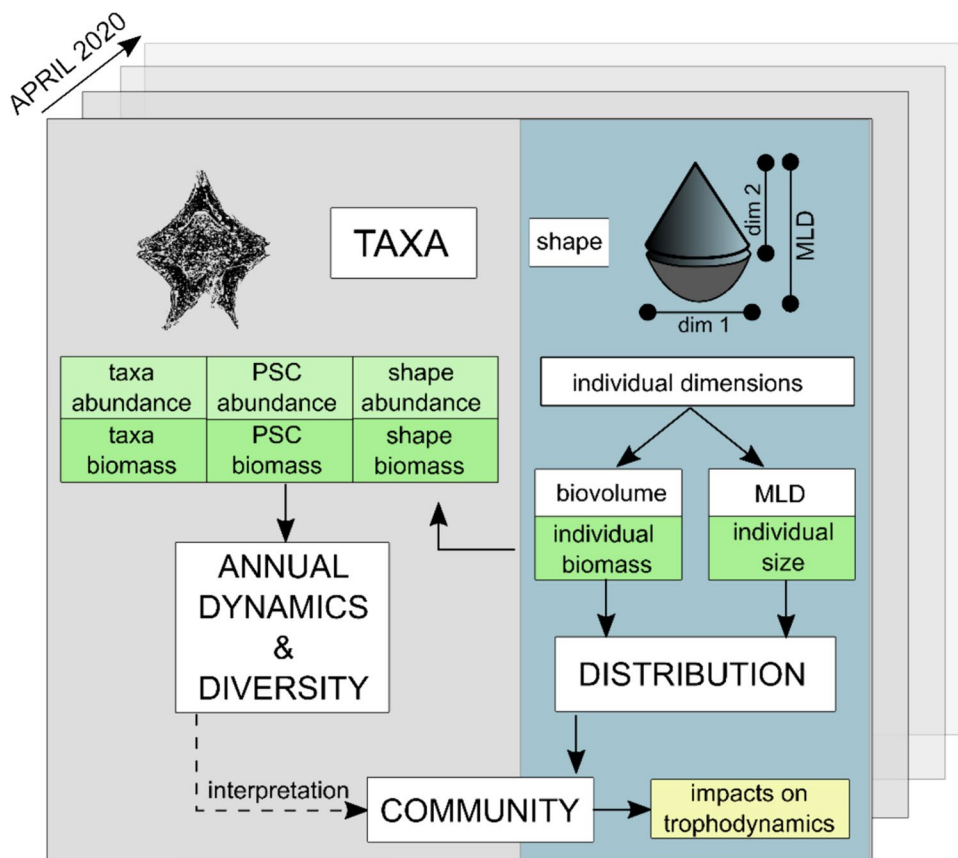
Referring to the cell size as maximum linear dimension (MLD), phytoplankton is usually classified in one of the three phytoplankton size classes (PSCs): picoplankton (0.2–2 μm), nanoplankton (2–20 μm) and microplankton (20–200 μm) (Sieburth et al., 1978). In the marine environment, the apportionment of biomass among PSCs is influenced by various biotic and abiotic factors, where, in general, the pico-fraction is advantaged at higher temperatures (Andersson et al., 1994), the nanofraction is advantaged at low nutrient concentrations, while microfraction is advantaged during nutrient pulses and in exploiting vertical gradients (Sommer et al., 2017). Also, the nanofraction is more affected by grazing by protists and

pelagic tunicates, while the microfraction is more affected by larger zooplanktonic grazers (Sommer et al., 2017).

In addition to size, other morphological, behavioural and physiological traits are important in defining the properties of resource acquisition and predator avoidance, namely mixotrophy, motility, shape, life forms (single cell vs. colony), and surface to volume ratio (Durante et al., 2019; Leonilde et al., 2017; Roselli & Litchman, 2017; Weithoff & Gaedke, 2016). In this context, cell shape not only plays a crucial role in defining the biomass of a cell, but also have an influence on the efficiency of resource utilization in phytoplankton as well (Ryabov et al., 2022). In fact, elongated shapes allow for a greater surface area to volume ratio, which maximizes nutrient uptake and improves chloroplast packing (Naselli-Flores & Barone, 2011). Shape irregularities in the form of spines, appendages and flagella (Sonnet et al., 2022) also prevent sinking, increase resistance to grazing and improve the displacement capacity of cells towards better nutrient and light conditions (Durante et al., 2019; Stanca et al., 2013). As a morpho-functional trait, shape is more effective than a simple taxonomic hierarchy in grouping ecologically similar species (Roselli et al., 2022) and, together with size, determine the morphological optimum for speciation and thus maximum diversity (Ryabov et al., 2022). The temporal dynamics of phytoplankton shape composition have been described as highly variable over the course of the year and without clear seasonality (Sonnet et al., 2022), but opposite results have been published as well (Stanca et al., 2013).

Estimates of phytoplankton cellular carbon based on time-consuming measurements of species biovolume are not routinely assessed in ecological time series in the area of interest (Gulf of Trieste, northern Adriatic Sea) and have been used only sporadically in studies on the partitioning of organic carbon among different compartments of the coastal ecosystem (Malej et al. 2003). In this work, we investigate the first annual time series of phytoplankton cell size and biomass by direct microscopic measurements, which were assessed at the level of total community, groups and individual cells (Fig. 1). In addition, we analysed the distributional properties of phytoplankton individual cell size (as MLD) and biomass and their consistency with the power law to infer the fate of phytoplankton biomass in the pelagic trophic interactions. To supplement this, we examined the diversity of taxa and their shape, which highlight important ecological processes and help interpret the trophodynamics since the trophic status and structure of the phytoplankton community in the Gulf of Trieste changed significantly after the turn of the century (Brush et al., 2021; Mozetič et al., 2012).

Fig. 1 Scheme of the relations between analysed phytoplankton parameters, the estimation methods, and objectives of the study. In green the parameters estimated in this study, in yellow the goals. (MLD=Maximum Linear Dimension; PSC=Phytoplankton Size Class)



Material and methods

The study area

The Gulf of Trieste (GoT) is a shallow basin surrounded by land at the north-eastern tip of the Adriatic Sea. This basin is very shallow (about 20 m on average) and is strongly influenced by meteorological conditions. The water column in the GoT is seasonally mixed and stratified (Malačič et al., 2006), and the euphotic zone considerably exceeds the depth of the upper mixed layer (Talaber et al., 2014). The sampling station 000F is located at the southern entrance of the GoT (Fig. 2) and represents the Slovenian long-term ecological research (LTER) site. The waters around the LTER station are generally crossed by the North Adriatic Dense Water (NAdDW) current and influenced by the river plume of the largest freshwater source in the GoT—the Soča (Isonzo) River (Fig. 2)(Zhang et al., 2020).

Phytoplankton exhibits strong seasonal fluctuations and large interannual variability in GoT and broader in the northern Adriatic (Brush et al., 2021; Totti et al., 2019). Usually, phytoplankton shows two seasonal peaks, first in late spring, which is inconstant and short-lived, and second larger and more constant in autumn (Vascotto et al., 2021). During blooms, phytoplankton community is mainly dominated by

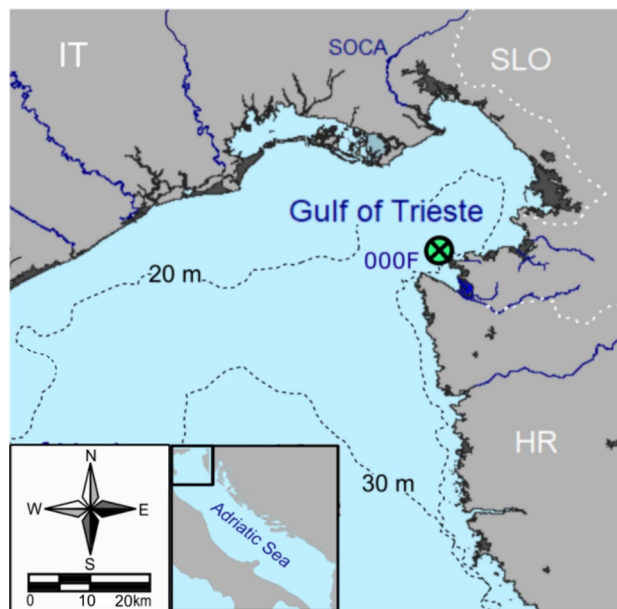


Fig. 2 Map of the study site: the sampling stations, 000F, represent the LTER site, Gulf of Trieste—Slovenia

diatoms, while during periods of low chlorophyll-a concentrations small cells (nanoflagellates, coccolithophores) prevail (Brush et al., 2021; Talaber et al., 2018). In this area, a trend towards oligotrophication and a decline in production has been observed in early 2000s (Mozetič et al., 2010), leading to the situation of low phytoplankton biomass strongly influenced by meteorological variability (Brush et al., 2021). Recently, more irregularity was observed in the formation of typical assemblages that was attributed to mesoscale climatic and hydrological drivers (Vascotto et al., 2021). Daily flows of the Soča River, measured approx. 45 km upstream, were downloaded from the web page of the Environmental Agency of the Republic of Slovenia (https://vode.arso.gov.si/hidarhiv/pov_arhiv_tab.php).

Biomass determination

Size, biovolume and cellular carbon

A year-long campaign of monthly sampling was conducted at sampling station 000F from April 2020 to March 2021. Phytoplankton samples were collected at the surface with Niskin bottles and fixed with neutralized formaldehyde. 50 ml of samples were then analysed with an inverted microscope ZEISS AxioObserver.Z1 using the Utermöhl method (Utermöhl, 1958), with either counting and measuring phytoplankton cells in a minimum of 100 fields at 400× magnification or alternatively counting and measuring 1000 phytoplankton cells in a sample. After examining the sample at 400× magnification, half sedimentation chamber was scanned at 100× magnification to check for bigger specimens. Phytoplankton cells were determined to the lowest taxonomic level possible and assigned to one of the main phytoplankton groups (diatoms, dinoflagellates, coccolithophores, silicoflagellates, cryptophytes, chlorophytes and unidentified phytoflagellates).

Currently, the most used method for estimating the biomass of a phytoplankton does not rely only on size, in fact, it is based on the assignment of each taxon to a three-dimensional shape (Olenina et al., 2006; Sun & Liu, 2003; Vadrucci et al., 2007). The dimensions of these shapes and the inferred biovolume and biomass are measured under the microscope, in parallel with taxonomic identification and enumeration. This method uses the formula of geometric models or shapes that most closely resemble the actual shape of the organism. During this process, one is often faced with the dilemma whether to assign the shape of a phytoplankton cell to a complex but similar geometric model or rather to a simple, easily measured but dissimilar shape (Sun & Liu, 2003). The importance of choosing the right shape formula is emphasized by the fact that due to the geometric relationship between size and volume, there is a wide range of nine

orders of magnitude for the cell biovolume of phytoplankton (Sutton, 1997).

To measure the biovolume, each phytoplankton species/taxon was first assigned to a shape according to the Helsinki Commission (HELCOM) classification system (Olenina et al., 2006) and found in the Nordic Microalgae website (Karlson et al., 2020). The taxa that were not present in the HELCOM list were assigned to the most similar shape and are, together with the complete list, reported in the Supplementary Materials (Table S1). Using ZEISS ZEN 3.0 software, the dimensions (length, width, diameter etc.) of each cell were measured individually, then the biovolume was calculated according to the formula assigned to a certain shape. When we found colonies in our samples, each cell of the colony was measured individually. The final biomass values (in pg C) were obtained using the Mendel-Deuer conversion factors (Menden-Deuer & Lessard, 2000; Socal et al., 2010). The size classes were obtained grouping the individual cell biomass and their abundances in the two classes (nano and micro) depending on their maximum linear dimension (MLD Fig. 1). Hereafter, to refer to the phytoplankton results measured by microscopy, the term Utermöhl phytoplankton will be used. The parameters measured in our study were taxa abundance (cell/L), shapes abundance (cell/L), taxa biomass (mg C /m³), shapes biomass (mg C /m³), individual cell biomasses (pg C), and individual cell sizes (MLD, µm) (Fig. 1).

Chlorophyll-a

The same monthly surface samples were used to determine chlorophyll-a (Chl-a) concentration. 400 mL of each sample was filtered through Whatman GF/F filters, and filters were frozen until analysis. Chl-a concentrations corrected for phaeopigments were then determined fluorometrically (Holm-Hansen et al., 1965) in 90% acetone extracts using a Turner Designs Trilogy fluorometer.

Analyses of data

The coherence among trends of different phytoplankton groups and among estimation methods was investigated using the Pearson determination coefficient (R^2) computed in the linear model II framework. The linear model II was obtained using the R package <lmodel2> (Legendre & Legendre, 2012). The differences among medians were tested using the nonparametric rank test based on quantiles from the R package <EnvStats.R>. The community diversity was calculated using the Shannon diversity index (H') with the R package <vegan.R> (Oksanen et al., 2018). For every month, the taxa biomass, taxa abundance, shape biomass and shape abundance were transformed in proportions. Each

contribution to the community compositions p_i was used in the equation below to obtain the diversity values.

$$H' = - \sum_{k=0}^n p_i \ln p_i$$

To test whether nano- and microplankton subpopulations formed two distinct distributions, the unimodality or bimodality of the distributions of log size and log biomass was tested using the method of (Hartigan & Hartigan, 1985) embedded in the R package <diptest.R> (Maechler et al., 2021). In case unimodality of a distribution was not met, the distribution was split into two using the Gaussian mixture models method of the R package <mclust.R> (Fraley et al., 2022). For each of resulting distributions (the original one in case of unimodality and the two split distributions in case of bimodality), the agreement with the power law was tested (bootstrap, Supplementary Material Figure S1). When the test results significant, the tested distribution is not a power law (p -value < 0.05); on the contrary, if the test results have a p -value > 0.05, then the distribution could be a power law or other similar distributions (exponential and lognormal) (Clauset et al. (2009). In case of p -value > 0.05, the lognormal and exponential distributions were tested against the power law using the method developed by Clauset et al.

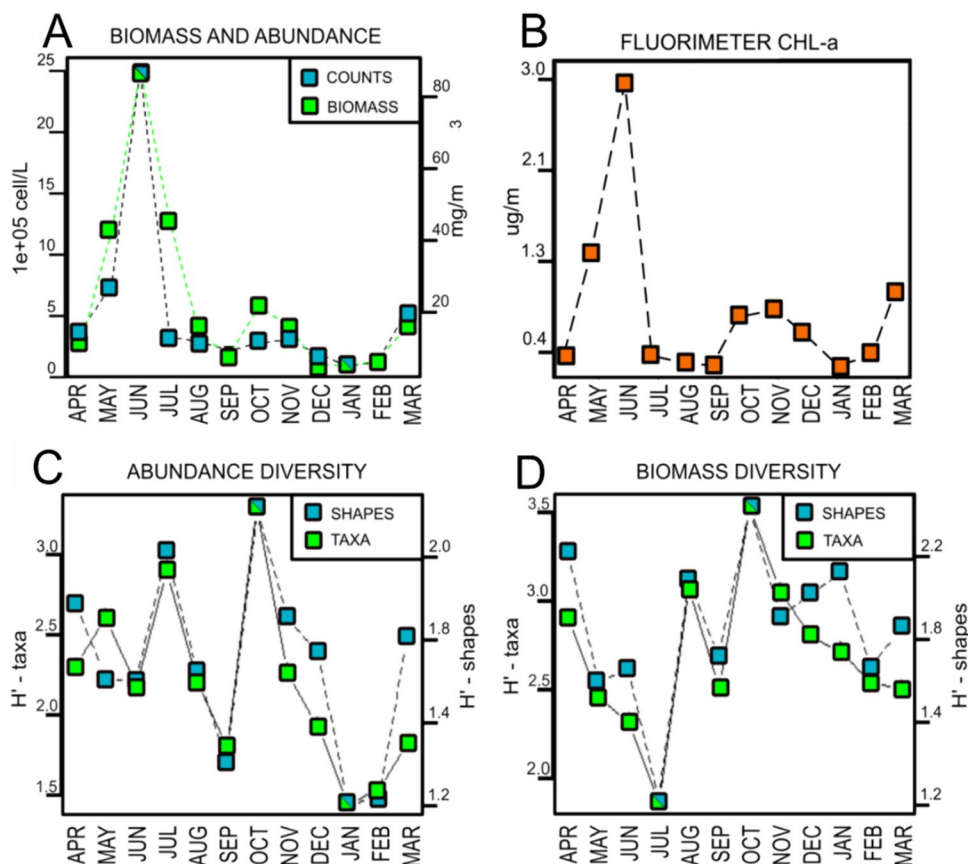
(2009), included in the <powerLaw.R> package (Gillespie, 2015). In case the test was not passed against one or both alternative distributions (exponential or power law), the support for the power law was considered as moderate, while in case both p -values were lower than 0.05, the support was considered as good. After Clauset et al. (2009), the support for power law was classified in “none”, “moderate” and “good”. The flowchart of the power law related analysis is schematized in the Supplementary Materials (Figure S1).

Results

Annual pattern of phytoplankton parameters

During the study period, a total of 10,030 cells were identified down to the lowest possible taxonomic level, counted and measured using an inverted microscope. The total abundance of phytoplankton exhibited three peaks (Fig. 3A). The highest abundance was observed in June 2020, while two minor peaks were observed in October–November 2020 and March 2021. The total carbon biomass followed the abundance pattern with very similar dynamics: the biomass peaked in June (89.4 mg C/m³).

Fig. 3 Annual pattern of phytoplankton characteristics at the station 000F in the period April 2020–March 2021. **A** abundance (left axis) and carbon biomass (right axis); **B** chlorophyll-a concentration; **C** Shannon diversity index calculated using abundance of taxa (left axis) and abundance of shapes (right axis); **D** Shannon diversity index calculated using biomass of taxa (left axis) and biomass of shapes (right axis)



Chl-a concentrations (Fig. 3B) peaked synchronously with total carbon biomass and abundance in June 2020, which was followed by a summer low. The second minor peak in November 2020 was again followed by a decline in late autumn and winter, when the concentration reached the low in January 0.21 mg/m^3 to then increase again in March 2021. The Chl-a concentrations were significantly correlated with total carbon biomass ($R^2=0.74$, p -value < 0.01).

Phytoplankton diversity, which was calculated based on the abundance of taxa (Fig. 3C), was fluctuating but with relatively high values during spring and summer and reached its maximum during the peak in October 2020 ($H' = 3.2$). The minimum diversity was calculated in January 2021 ($H' = 1.7$) and was also low in September 2020. Very similar was the pattern of diversity calculated with the abundance of cell shapes ($R^2=0.76$, p -value $= < 0.01$), which slightly differed only in April–May 2020 and March 2021. Phytoplankton diversity based on the carbon biomass of taxa displayed a different temporal pattern (Fig. 3D). It decreased from high values in April 2020 and reached its minimum in July ($H' = 2.0$). The trend then reversed, and diversity peaked again in August and October 2020 (up to $H' = 3.5$), only to decline again in the winter months. Similar pattern was also observed for the diversity calculated with carbon biomass of different cell shapes ($R^2=0.83$, p -value $= < 0.01$). The autumn peak in phytoplankton abundance and carbon biomass, recorded in October/November, corresponded to the maximum in shape diversity for both shape abundance ($H' = 2.36$) and biomass ($H' = 2.16$).

The June and October/November peaks were characterized by an increase in the median of the individual cell sizes, while the March peak corresponded to a non-significant

decrease (p -value > 0.05) (Fig. 4 and Supplementary Material Table S2). From the perspective of individual cell biomass, only the October/November period was characterized by an increase in average values while the March peak was characterized by a significant decrease (Fig. 4 and Supplementary Material Table S2). Both June and October peaks were preceded by an increase in freshwater inputs from the main river while the March peak was accompanied by a significant decrease in freshwater inputs (Supplementary Material Figure S2 and Table S2).

Phytoplankton size classes and main taxa

Phytoplankton size classes contributed differently to the community with respect to biomass and abundance. Microfraction (MLD $> 20 \mu\text{m}$) accounted for an average of 60% of the Utermöhl phytoplankton biomass, while nanofraction (MLD $2 - 20 \mu\text{m}$) accounted for the remaining (Supplementary Material Table S3). Microphytoplankton share in the carbon biomass rose during the peaks to almost 90% in July 2020 and up to 80% in November 2020. The contribution of nanophytoplankton biomass was the highest during early spring (up to 72% in April 2020) and in December 2020 (71%). As expected, much higher contribution accounted for nanophytoplankton in case of abundance (Supplementary Material Table S4), where it accounted for an average of 80% of the total abundance. The contribution of microphytoplankton abundance was the highest during peaks (up to 30% in June and July and up to 44% in November).

The community composition in terms of phytoplankton main groups was during peaks characterized by the prevalence of diatoms, which dominated both in biomass (up to

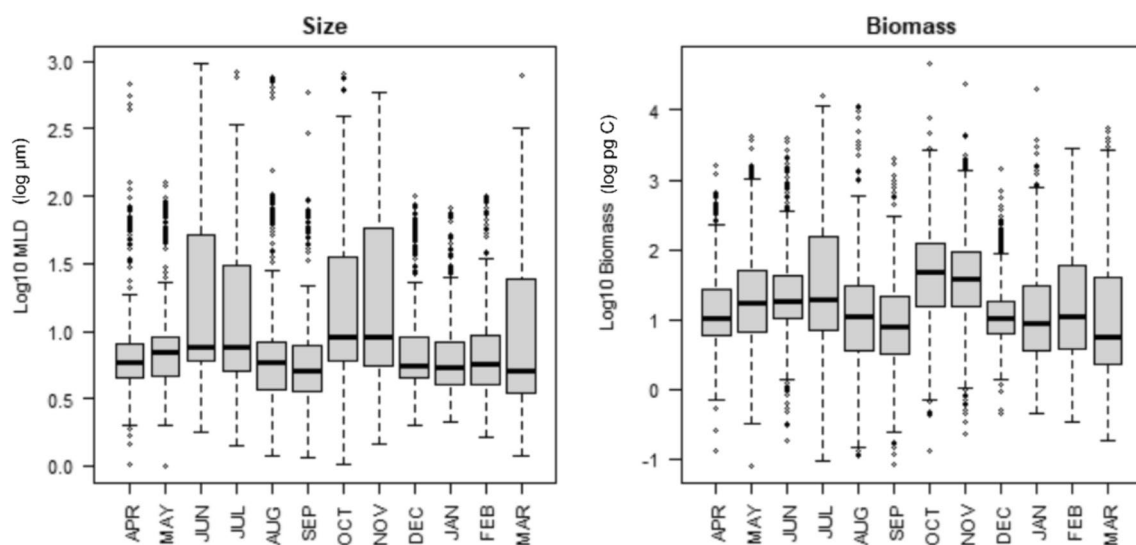
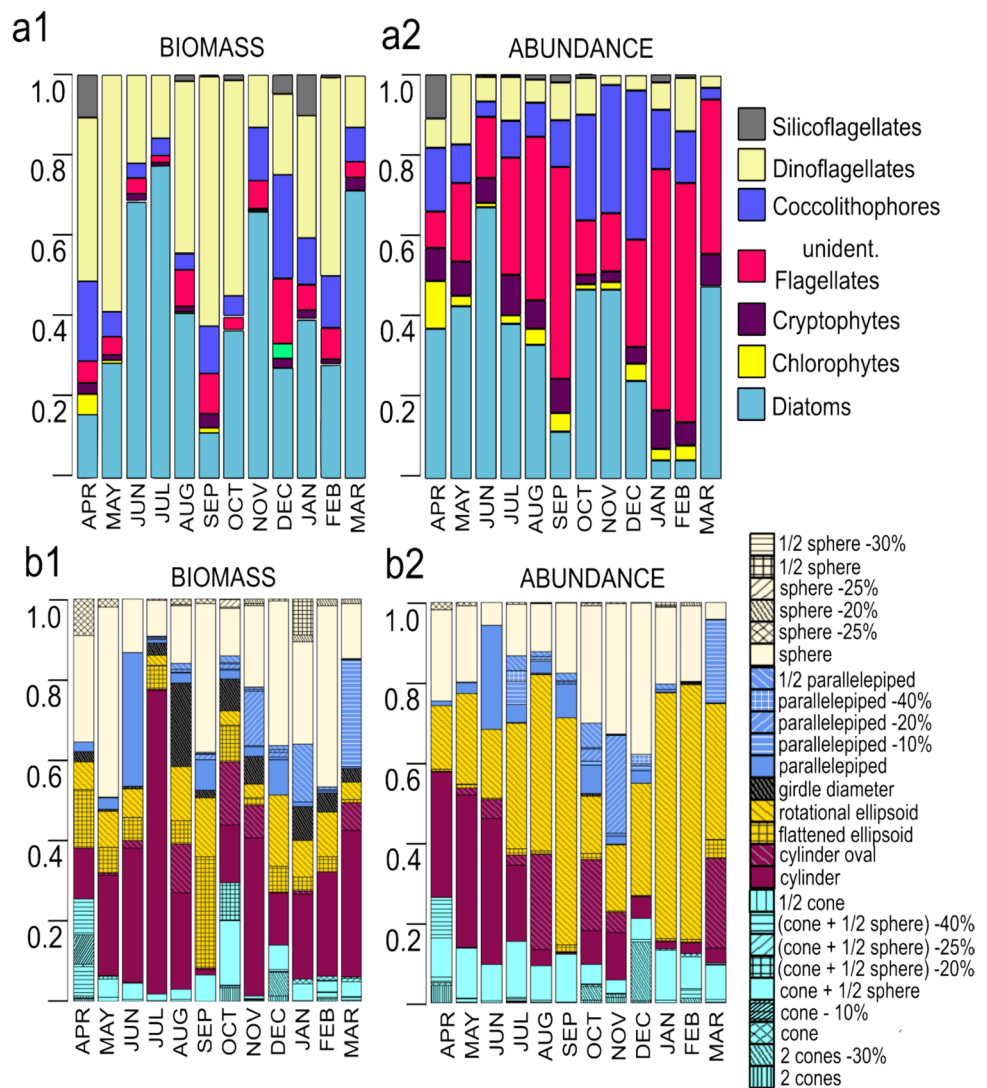


Fig. 4 Annual pattern of individual phytoplankton cell size (in terms of MLD; left) and biomass (in terms of carbon biomass; right) at the station 000F in the period April 2020–March 2021

Fig. 5 Phytoplankton community composition at the station 000F in the period April 2020–March 2021: **a1** contribution of main groups to total biomass, **a2** contribution of main groups to total abundance; **b1** contribution of shapes to total biomass, **b2** contribution of shapes to total abundance



77%; Fig. 5a1) and abundance (up to 68%; Fig. 5a2). The share of dinoflagellates was, on the other hand, the highest during non-bloom periods, but only in terms of biomass (up to 55% in September; Fig. 5a1), while the non-bloom periods were dominated by flagellates in terms of abundance (up to 60%; Fig. 5a2). Coccolithophore share to abundance was the most important during autumn months (up to 37%; Fig. 5a2). Unidentified nanoflagellates and coccolithophores together with cryptophytes accounted for less biomass than dinoflagellates alone. Other groups had minor contributions for the total phytoplankton abundance and biomass (Fig. 5 and Supplementary Material Tables S3 and S4). The most uniform contribution of phytoplankton groups to the community was observed in the periods of the lowest biomass (April and December, Fig. 5).

Total carbon biomass and abundance were significantly correlated ($R^2=0.82$, p -value <0.01), which was also mostly true when separately considering main phytoplankton

groups. For cryptophytes and chlorophytes, biomass correlated almost perfectly with abundance (R^2 close to 1), and for dinoflagellates, correlation was also quite high ($R^2=0.86$, p -value <0.01). For diatoms, the correlation was positive but not significant as it was strongly driven by the June peak ($R^2=0.77$, p -value >0.01), and for the coccolithophores, the correlation was lower but nonetheless significant ($R^2=0.60$, p -value <0.01). Biomass and abundance were positively correlated also for both PSCs (micro-size class $R^2=0.69$, p -value <0.01 ; nanosize class $R^2=0.89$, p -value <0.01).

Phytoplankton cell shapes

During the study period, 25 different shapes were registered that can be divided in six groups: nine shapes closely related to cones, two cylinders, two ellipoids, five parallelepipeds, six spheres, and one unique shape of the genus *Tripos*, denoted as girdle diameter. In general, individual cell size

and individual biomass of phytoplankton cells were significantly correlated ($R^2=0.53$, p -value < 0.01). However, this correlation was stronger for spheres, ellipsoids and girdle diameter ($R^2=0.81$, 0.91 and 1.00 , respectively) than for cylinders, parallelepipeds and cones ($R^2=0.77$, 0.20 and 0.10 , respectively). The shape influenced the relation between total abundance and biomass as well. In fact, depending on the shape type, the correlation was stronger (parallelepipeds, ellipsoids and spheres $R=0.99$, 0.77 , 0.68 , respectively) or weaker (girdle, cylinders and cones $R^2=0.47$, 0.42 , 0.30 , respectively).

There was substantial variation in the dominance of different shapes during the study period (Fig. 5b1, b2 and Supplementary Material Tables 5 and 6). Cylinders and parallelepipeds, associated with diatoms, dominated the abundance (41% and 26%, respectively) and biomass (35 and 33%, respectively) peak in June 2020, and their contribution was quite similar also during smaller March 2021 peak. Differently, all shapes contributed more or less uniformly to the autumn peak, especially in October 2020. The contribution of cylinders to biomass was the highest in months following the phytoplankton peaks July and November 2020 (75 and 39%, respectively), while their contribution to the abundance during these months was much smaller. In the months with the phytoplankton lows, both biomass and abundance were dominated by ellipsoids (up to 42% of biomass in September 2020) and spheres (up to 45% of biomass in February 2021 and 38% of abundance in December 2020). In absolute terms, spherical shapes reached their maximum biomass and abundance in May 2020, when their contribution to biomass also peaked (47%). The contribution of the genus *Triplosira* shape denominated girdle diameter to biomass was very variable, reaching the peak in August 2020 (21%), while its contribution to the abundance was negligible.

Distributions of individual cell size and biomass

The phytoplankton cell size in terms of MLD ranged from 2 to 821.5 μm . The largest cells in each sample belonged to diatoms. The carbon biomass of individual phytoplankton cells ranged from 0.08 to 46,529 pg C. In contrast to the linear dimension, the majority of taxa with the highest carbon biomass belonged to the dinoflagellates, with one specimen of *Protoperidinium depressum* having the highest biomass. The distributions of phytoplankton individual cell sizes passed the Hartigan test for unimodality in only four cases: April and September 2020, January, and February 2021, which corresponds to periods of the lowest total biomass and abundance (see Fig. 3A). For these months, a unique average cell size was estimated, which varied between 7 and 11 μm MLD (one solid vertical line in Fig. 6 and Supplementary material Table 9). In other months, the individual cell size was characterized by a bimodal distribution. In

these months, the average cell size in the subpopulation of smaller cells ranged from around 5 to 7 μm MLD, whereas the average cell size in the subpopulation of larger cells was more variable and ranged from 18 to 78 μm MLD (Fig. 6, Supplementary material Table S7). Only the distributions of November 2020, December 2020, and February 2021 as well as the subpopulation of larger cells in May 2020 and smaller cells in June 2020 conformed to a power law (p -value > 0.05 ; Supplementary material Table S7). Of these, only the distributions of the small cells in June, November and December did not conform to the alternative distributions, i.e. lognormal and exponential (p -value < 0.05), indicating a good support for power law.

The distributions of individual cell biomass did not pass the Hartigan test for unimodality only in June, July and October 2020, and March 2021 (two dashed vertical lines in Fig. 6 and Supplementary material Table S7), which corresponds to months of phytoplankton biomass peaks. Only the distributions of April, January, and February and the small cells in June conformed to a power law distribution (p -value > 0.05 ; Supplementary material Table S7). For all three, it was not possible to discriminate the distribution from at least one of the two alternative distributions (p -value > 0.05 ; Supplementary material Table S7) indicating a moderate support for power law.

Discussion

In this paper, we present an annual characterization of the phytoplankton community in terms of taxonomy (main groups), morphology (size and shape) and diversity, which, in combination with their distributional properties, allows conclusions to be drawn about the ecology of the pelagic community at the LTER site in the Gulf of Trieste (northern Adriatic Sea). Our results on phytoplankton size (MLD), biovolume and biomass add to the total of around 40 such datasets found worldwide (Harrison et al., 2015) and are, to the best of our knowledge, one of the few existing for the Mediterranean Sea.

The general pattern of two annual peaks of phytoplankton abundance and biomass, one in the spring and one in the autumn, match with the known phytoplankton phenology in the Gulf of Trieste, where seasonal outbursts are associated with water column freshening and mixing (Cabrinini et al., 2012; Cerino et al., 2019; Mozetič et al., 2012). The late appearance of spring phytoplankton peak during our study is also consistent with findings in this area, where late spring to summer diatom-dominated blooms recently substituted late winter or spring blooms (Cerino et al., 2019; Eker-Develi et al., 2022; Godrijan et al., 2013; Mozetič et al., 2012). Moreover, the minor relative importance of the autumn bloom is consistent with recent changes of phytoplankton

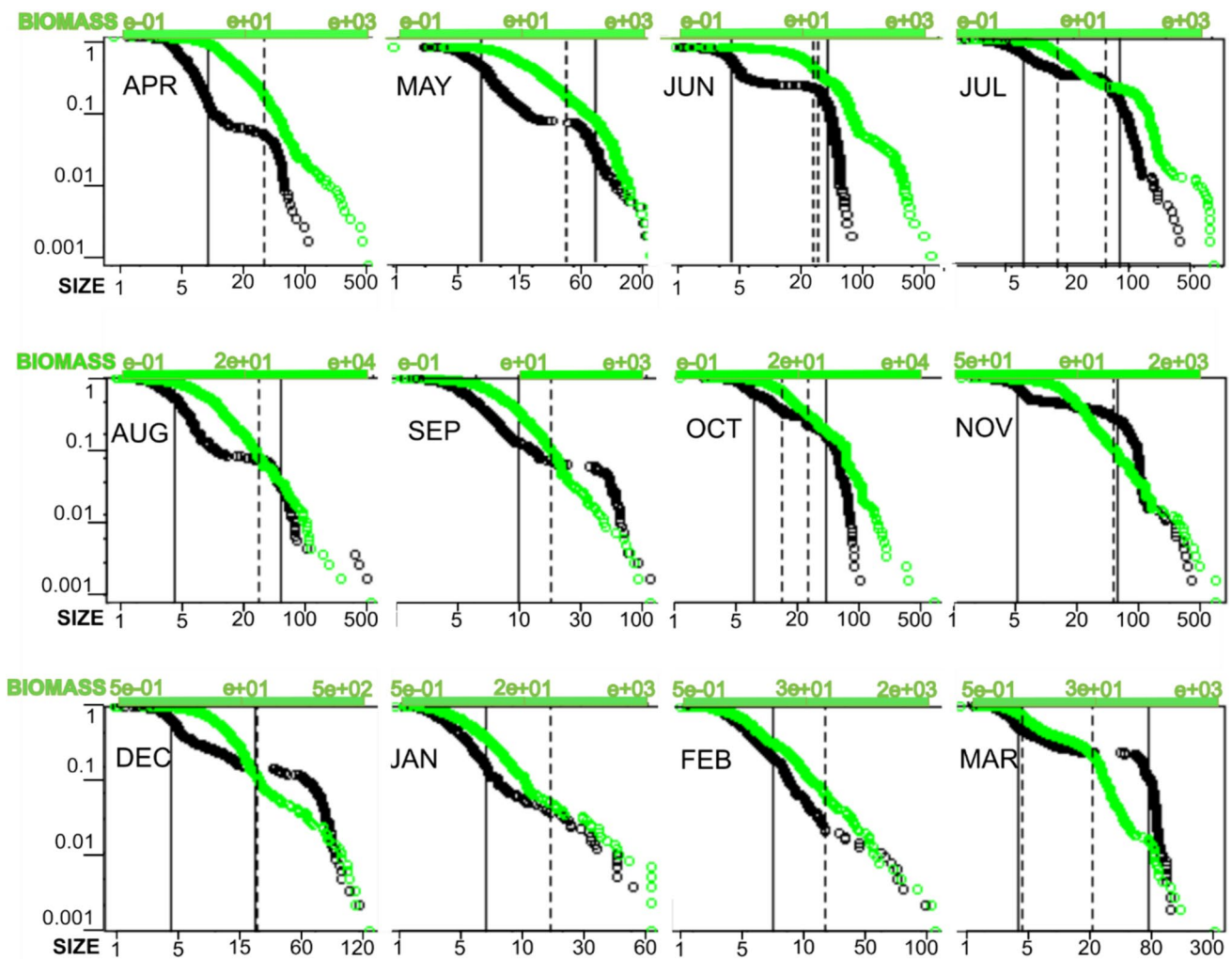


Fig. 6 Log–log cumulative distribution plots for individual cell size (in μm , black dots) and individual cell biomass (in pg C , green dots). The solid vertical line represents the average size, if there are two lines, they represent the average size of the two subpopulations. The

dashed vertical line represents the average biomass; when there are two lines, they represent the average biomass of the two subpopulations. Note the different scale on x axes

annual dynamics, as either the biomass (in terms of Chl-a) or the abundances of main phytoplankton groups diminished after the break of the century (Brush et al., 2021). The community appeared to be more diverse during the autumn peak both functionally (shapes) and taxonomically in comparison to the spring period, which can be explained by the mechanisms causing the blooms. In the study area, the spring season is characterized by a stratified water column caused mainly by freshwater inputs, which enrich the surface layer with nutrients and cause diatom blooms mostly dominated by a small number of species (Brush et al., 2021). In autumn season, mixed conditions prevail, which redistribute nutrients from deeper water layers (Vascotto et al., 2024) and allow for a more complex and diverse community compared to other seasons (Vascotto et al., 2021). Active mixing can also favour the diversity by bringing specimens from the

deeper layers into the surface, which was sampled in this study. Such an increase in diversity could also reflect the accumulation of species at the end of the phytoplankton succession cycle (Reynolds, 1980).

The range of cellular carbon of the Utermöhl phytoplankton ($2.5\text{--}89\text{ mg C/m}^3$) is similar to that found in the eutrophic western part of the northern Adriatic (Bernardi Aubry et al., 2006; Pugnetti et al., 2008), while the values in the southern Adriatic are much lower (Cerino et al., 2012). This is consistent with the known gradient of increasing phytoplankton biomass along the south–north axis of the Adriatic Sea (Bernardi Aubry et al., 2006; Fonda Umani, 1996). Since our data cover only the surface layer, it is not possible to draw conclusions about the dynamics of phytoplankton in the lower water layers. In the Gulf of Trieste, in particular, the dynamics of the biomass in the lower layers are different

from the surface during the stratified water column (Flander-Putrlle et al., 2021; Talaber et al., 2014).

Depending on the taxa and their shape, the relation between individual size and individual biomass as well as the relation between total abundance and biomass showed different degrees of coherence. The significant correlation between phytoplankton abundance and biomass suggests the possibility of using abundance data as a proxy for biomass, and size (MLD) as a parameter (or trait) to estimate the individual biomass (Hillebrand et al., 1999). Although similar matchups for the marine environment between biomass and abundance have already been obtained before (Bernardi Aubry et al., 2006), there are also cases where satisfying agreement between the two parameters has not been achieved (Eker-Develi et al., 2022). Still, the output of this more demanding method, i.e. individual cell size, shape and biomass, can tell us other valuable information on the status and fit of the phytoplankton community in relation to energy flow, carbon export and carbon pump (Juranek et al., 2020). However, the major drawback when using Utermöhl method is the neglect of the pico-fraction. A previous study on PSCs based on HPLC pigments in GoT has shown that the pico-fraction makes the highest contribution (up to 30%) to the total biomass in the periods with the lowest Chl-a concentration. This contribution can be up to 30% of the total Chl-a in August and January, when cyanobacteria and chlorophytes predominate, respectively (Flander-Putrlle et al., 2021). The relative importance of picophytoplankton may even increase in the future, as the biomass of picophytoplankton has recently increased significantly in all water layers of the GoT (Flander-Putrlle et al., 2021).

The distributions of individual cell size and biomass were quite variable during the study period and often presented a mismatch between the size (MLD) and biomass suggesting nonlinear relationship between the two traits. This mismatch was also depicted by the results of the distribution tests (see Supplementary Material Table S7). It has to be stressed, however, that the power law test cannot perform at its best when the tested distribution does not span several orders of magnitude (Clauset et al., 2009), as was the case for the cell size subpopulations in our study. More specifically, for the size subpopulations of May, June, November and December that passed the test, special care must be taken before claiming that the distributions really corresponded to a power law. Nevertheless, two important characteristics can be drawn from the results: (i) unimodality was more common during periods of low phytoplankton biomass and abundance, meaning that phytoplankton community size and biomass could be described by one average value, and (ii) bimodality was more common during peaks, when more than one average value of biomass and size have to be used for describing the community. Moreover, the unimodal individual cell biomass distributions in the months with lower biomass (April,

January and February) showed tendency to the power law, while during the months with higher biomass characterized by bi- or even tri-modality, the individual cell biomass distributions mostly conformed to other types of curves (log-normal or exponential) and only once to power law.

Apart from temporal differences between distributions, it is important to note that bimodality was a more common characteristic of the individual cell size (MLD) while unimodality was more frequent for individual cell biomass. Bimodality of individual cell size support the “classic” division of Utermöhl phytoplankton into nano- and micro-size classes, but specific variations during the study period indicate different underlying ecological processes. For example, November 2020 showed a distinct second change in slope in the range between 100 and 500 μm (see Fig. 6), indicating a possible third mode of distribution in the mesoplankton size class/or fraction. Indeed, big cylindrical cells of diatoms from the genera *Guinardia*, *Pseudosolenia*, *Hemiaulus* and *Rhizosolenia* were present in that period along with other diatoms in the micro-size fraction, most probably in relation to favourable conditions of a mixed nutrient enriched water column (Svensson et al., 2014) that allowed a highly diversified autumn community (see Fig. 5). Conversely, in the cases where the distribution of individual cell size was unimodal during periods of low phytoplankton biomass and abundance (i.e. in April, September, January and February), the community was dominated by nano-sized phytoplankton. In such cases, the distinction between nanoplankton and microplankton is hardly seen in data and appears to be more of an artefact than a meaningful ecological trait.

On the contrary, the biomass of individual cells was either uniformly (when the power law applies) or unimodally distributed in most cases, except in peak periods when two (October 2020) or even three (June, July 2020 and March 2021) subpopulations were present as shown by the cumulative distribution plots of biomass (see Fig. 6). Our results show that phytoplankton biomass in coastal waters deviates very often from the power law, not only in correspondence to the seasonal blooms. Indeed, the assumption of energy flow from smaller to larger organisms, which characterize the food networks resulting in power law distributions, does not hold for the size spectrum occupied by phytoplankton (Witek & Krajewska-Soltys, 1989). More specifically, phytoplankton biomass can grow exponentially when unimpeded by grazers in coastal waters (Irigoiien et al., 2005), which deforms the expected power law distribution for the whole plankton range (Witek & Krajewska-Soltys, 1989). Similar results were obtained in our study, where size-specific blooms caused deviations from the power law inside the phytoplankton size spectrum itself (e.g. predominant cylinder and parallelepiped shapes characteristic for diatoms during June-July bloom).

The alternation between the bimodally and the unimodally power law distributed communities reflects the seasonal switches between unconstrained and constrained phytoplankton growth. In the first case, when the GoT is influenced by a high river discharge, the phytoplankton community is characterized by high biomass, bigger cells, clear separation between size classes, and higher contribution of diatoms in the microplankton size fraction. Such communities are richer in taxa and more diverse in terms of cell shapes, which indicates functional differentiation, especially in autumn. It has been argued that phytoplankton blooms, or peaks in our case, can be considered trophic “loopholes” as phases in the phytoplankton life cycles when species can proliferate exponentially unconstrained (Irigoien et al., 2005). During phytoplankton peaks, biomass increases in a specific range that is characteristic of the blooming taxa causing the deviation of the overall distribution of individual cell biomass from the power law.

Conversely, in more oligotrophic conditions, the phytoplankton community is characterized by smaller cells with a lower biomass, no clear separation between size classes, lower diversity, and a higher contribution of pico- and nanofractions. These communities, in which distributions of individual cell size and biomass more often conform to the power law, appear during lower freshwater outflows and during winter. Apart from scarce resources (nutrient and light availability), grazers like microzooplankton and heterotrophic nanoflagellates with similar growth rates to those of phytoplankton exert top-down control, maintaining phytoplankton biomass at low levels (Monti et al., 2012). Such communities can be considered in the final stage of a stable food web, which is organized in trophic networks that exhibits self-organized criticality (Bascompte, 2007) implying distributions conforming to the power law (Newman, 2005). In other words, in the post-bloom period where there are less resources available, grazers can “catch up” leading phytoplankton biomass to decrease and the distribution of individual cell biomass returns to the power law. These outcomes suggest that analyses of the distribution types of individual cell size and biomass can be seen as a useful tool to identify imbalances in the trophic network also in the coastal environment.

Conclusions

In this paper, we present a comprehensive characterization of the morphological traits (size and shape) and biomass of phytoplankton at the LTER site in the Gulf of Trieste (northern Adriatic Sea), which provided an insight into ecological processes driving the evolution of the phytoplankton community in time. Overall, the observed annual pattern of total phytoplankton abundance, carbon biomass and chlorophyll-a

corresponded well to the expected phytoplankton dynamics in this area. The individual cell size distributions confirmed the subdivision of the phytoplankton community into nano- and micro-size fraction, especially in the periods during and around the abundance and biomass peaks. In contrast, the distribution of individual cell biomass was more often unimodal except during the peaks, showing that the biomass of phytoplankton cells usually presents a continuum. The conformity of the biomass distribution to the power law in the months of low biomass indicates a link to stable trophic networks controlled by consumers and resources, while the more frequently observed deviations reflect the unstable nature of the coastal environment driven by the irregular pulses of freshwater inflows.

Supplementary Information The online version contains supplementary material available at <https://doi.org/10.1007/s42974-024-00215-4>.

Funding Open access funding provided by Istituto Nazionale di Oceanografia e di Geofisica Sperimentale within the CRUI-CARE Agreement. This research was funded by Slovenian Research and Innovation Agency (ARIS), grant number P1-0237, and by the ARIS programme for young researcher 51986.

Data availability Part of data (chlorophyll-a) originates from the national monitoring programme financed by the Slovenian Environment Agency of the Ministry of Environment and Spatial Planning. The Soča River discharge data is available at https://vode.arso.gov.si/hidarhiv/pov_arhiv_tab.php.

Declarations

Conflict of interest The authors declare that they have no known competing financial interests or personal relationships that could have appeared to influence the work reported in this paper.

Open Access This article is licensed under a Creative Commons Attribution 4.0 International License, which permits use, sharing, adaptation, distribution and reproduction in any medium or format, as long as you give appropriate credit to the original author(s) and the source, provide a link to the Creative Commons licence, and indicate if changes were made. The images or other third party material in this article are included in the article's Creative Commons licence, unless indicated otherwise in a credit line to the material. If material is not included in the article's Creative Commons licence and your intended use is not permitted by statutory regulation or exceeds the permitted use, you will need to obtain permission directly from the copyright holder. To view a copy of this licence, visit <http://creativecommons.org/licenses/by/4.0/>.

References

- Andersen, K. H., Berge, T., Goncalves, R. J., Hartvig, M., Heuschele, J., Hylander, S., Jacobsen, N. S., Lindemann, C., Martens, E. A., Neuheimer, A. B., Olsson, K., Palacz, A., Prowe, A. E., Sainmont, J., Traving, S. J., Visser, A. W., Wadhwa, N., & Kiorboe, T. (2016). Characteristic sizes of life in the oceans, from bacteria to whales. *Annual Review of Marine Science*, 8, 217–241.
- Andersson, A., Haecky, P., & Hagström, A. (1994). Effect of temperature and light on the growth of micro- nano- and pico-plankton: impact on algal succession. *Marine Biology*, 120(4), 511–520.

- Armstrong, R. A. (1999). Stable model structures for representing biogeochemical diversity and size spectra in plankton communities. *Journal of Plankton Research*, 21(3), 445–464.
- Aumont, O., Ethé, C., Tagliabue, A., Bopp, L., & Gehlen, M. (2015). PISCES-v2: An ocean biogeochemical model for carbon and ecosystem studies. *Geoscientific Model Development*, 8(8), 2465–2513.
- Bascompte, J. (2007). Networks in ecology. *Basic and Applied Ecology*, 8(6), 485–490.
- Beardall, J., Allen, D., Bragg, J., Finkel, Z. V., Flynn, K. J., Quigg, A., Rees, T. A. V., Richardson, A., & Raven, J. A. (2009). Allometry and stoichiometry of unicellular, colonial and multicellular phytoplankton. *New Phytologist*, 181(2), 295–309.
- BernardiAubry, F., Acri, F., Bastianini, M., Bianchi, F., Cassin, D., Pugnetti, A., & Socal, G. (2006). Seasonal and interannual variations of phytoplankton in the Gulf of Venice (Northern Adriatic Sea). *Chemistry and Ecology*, 22(sup1), S71–S91.
- Brown, J. H. (2004). Toward a metabolic theory of ecology. *Ecology*, 85(7), 1771–1789.
- Brush, M. J., Mozetič, P., Francé, J., Aubry, F. B., Djakovac, T., Faganelli, J., Harris, L. A., & Niesen, M. (2021). *Phytoplankton dynamics in a changing environment*. Wiley.
- Cabrini, M., Fornasaro, D., Cossarini, G., Lipizer, M., & Virgilio, D. (2012). Phytoplankton temporal changes in a coastal northern Adriatic site during the last 25 years. *Estuarine, Coastal and Shelf Science*, 115, 113–124.
- Cavender-Bares, K. K., Rinaldo, A., & Chisholm, S. W. (2001). Microbial size spectra from natural and nutrient enriched ecosystems. *Limnology and Oceanography*, 46(4), 778–789.
- Cerino, F., BernardiAubry, F., Coppola, J., La Ferla, R., Maimone, G., Socal, G., & Totti, C. (2012). Spatial and temporal variability of pico-, nano- and microphytoplankton in the offshore waters of the southern Adriatic Sea (Mediterranean Sea). *Continental Shelf Research*, 44, 94–105.
- Cerino, F., Fornasaro, D., Kralj, M., Giani, M., & Cabrini, M. (2019). Phytoplankton temporal dynamics in the coastal waters of the north-eastern Adriatic Sea (Mediterranean Sea) from 2010 to 2017. *Nature Conservation*, 34, 343–372.
- Clauset, A., Shalizi, C. R., & Newman, M. E. J. (2009). Power-law distributions in empirical data. *SIAM Review*, 51(4), 661–703.
- Durante, G., Basset, A., Stanca, E., & Roselli, L. (2019). Allometric scaling and morphological variation in sinking rate of phytoplankton. *Journal of Phycology*, 55(6), 1386–1393.
- Eker-Develi, E., Berthon, J.-F., & Free, G. (2022). Impact of environmental factors on phytoplankton composition and their marker pigments in the northern Adriatic Sea. *Oceanologia*, 64(4), 615–630.
- Falkowski, P. G., Laws, E. A., Barber, R. T., & Murray, J. W. (2003). "Phytoplankton and their role in primary, new, and export production. In J. Michael and R. Fasham (Eds.), *Ocean biogeochemistry* (pp. 99–121). Springer.
- Finkel, Z. V., Beardall, J., Flynn, K. J., Quigg, A., Rees, T. A. V., & Raven, J. A. (2009). Phytoplankton in a changing world: Cell size and elemental stoichiometry. *Journal of Plankton Research*, 32(1), 119–137.
- Flander-Putrlle, V., Francé, J., & Mozetič, P. (2021). Phytoplankton pigments reveal size structure and interannual variability of the coastal phytoplankton community (Adriatic Sea). *Water*, 14(1), 23.
- Fonda Umani, S. (1996). Pelagic production and biomass in the Adriatic Sea. *Scientia Marina*, 60(2), 65–77.
- Fraley, C., Raftery, A. E., Scrucca, L., Murphy, T. B., & Fop, M. (2022). *Gaussian mixture modelling for model-based clustering, classification, and density estimation*. Chapman and Hall.
- Gillespie, C. S. (2015). Fitting heavy tailed distributions: The power-law package. *Journal of Statistical Software*. <https://doi.org/10.18637/jss.v064.i02>
- Godrijan, J., Marić, D., Tomažič, I., Precali, R., & Pfannkuchen, M. (2013). Seasonal phytoplankton dynamics in the coastal waters of the north-eastern Adriatic Sea. *Journal of Sea Research*, 77, 32–44.
- Harrison, P. J., Zingone, A., Mickelson, M. J., Lehtinen, S., Ramaiah, N., Kraberg, A. C., Sun, J., McQuatters-Gollop, A., & Jakobsen, H. H. (2015). Cell volumes of marine phytoplankton from globally distributed coastal data sets. *Estuarine, Coastal and Shelf Science*, 162, 130–142.
- Hartigan, J. A., & Hartigan, P. M. (1985). The dip test of unimodality. *The Annals of Statistics*, 13(1), 70–84.
- Hatton, I. A., Heneghan, R. F., Bar-On, Y. M., & Galbraith, E. D. (2021). The global ocean size spectrum from bacteria to whales. *Science Advances*. <https://doi.org/10.1126/sciadv.abh3732>
- Hays, G. C., Richardson, A. J., & Robinson, C. (2005). Climate change and marine plankton. *Trends in Ecology & Evolution*, 20(6), 337–344.
- Heneghan, R. F., Hatton, I. A., & Galbraith, E. D. (2019). Climate change impacts on marine ecosystems through the lens of the size spectrum. *Emerg Top Life Sci*, 3(2), 233–243.
- Hillebrand, H., Dürselen, C. D., Kirschtel, D., Pollinger, U., & Zohary, T. (1999). Biovolume calculation for pelagic and benthic microalgae. *Journal of Phycology*, 35(2), 403–424.
- Holm-Hansen, O., Lorenzen, C. J., Holmes, R. W., & Strickland, J. D. (1965). Fluorometric determination of chlorophyll. *ICES Journal of Marine Science*, 30(1), 3–15.
- Irigoién, X., Flynn, K. J., & Harris, R. P. (2005). Phytoplankton blooms: A 'loophole' in microzooplankton grazing impact? *Journal of Plankton Research*, 27(4), 313–321.
- Juranek, L. W., White, A. E., Dugenne, M., Henderikx Freitas, F., Dutkiewicz, S., Ribalet, F., Ferrón, S., Armbrust, E. V., & Karl, D. M. (2020). The importance of the phytoplankton "middle class" to ocean net community production. *Global Biogeochemical Cycles*, 34(12), e2020GB006702.
- Karlson, B., A. Andreasson, M. Johansen, M. Karlberg, A. Loo and A.-T. Skjevik. (2020). Nordic microalgae. [World-wide electronic publication](http://nordicmicroalgae.org), from <http://nordicmicroalgae.org>.
- Kostadinov, T. S., Siegel, D. A., & Maritorena, S. (2009). Retrieval of the particle size distribution from satellite ocean color observations. *Journal of Geophysical Research*. <https://doi.org/10.1029/2009JC005303>
- Kostadinov, T. S., Siegel, D. A., & Maritorena, S. (2010). Global variability of phytoplankton functional types from space: Assessment via the particle size distribution. *Biogeosciences*, 7(10), 3239–3257.
- Kriest, I., & Evans, G. T. (1999). Representing phytoplankton aggregates in biogeochemical models. *Deep-Sea Research*, 46(1), 1841–1859.
- Legendre, P., & Legendre, L. (2012). *Numerical ecology*. Elsevier.
- Leonilde, R., Elena, L., Elena, S., Francesco, C., & Alberto, B. (2017). Individual trait variation in phytoplankton communities across multiple spatial scales. *Journal of Plankton Research*, 39(3), 577–588.
- Litchman, E., & Klausmeier, C. A. (2008). Trait-based community ecology of phytoplankton. *Ann. Rev. Ecol. Evol. Syst.*, 39(1), 615–639.
- Maechler, M., P. Rousseeuw, A. Struyf, M. Hubert and K. Hornik. (2021). Cluster: Cluster analysis basics and extensions.
- Malačić, V., Celio, M., Čermelj, B., Bussani, A., & Comici, C. (2006). Interannual evolution of seasonal thermohaline properties in the Gulf of Trieste (northern Adriatic) 1991–2003. *Journal of Geophysical Research*. <https://doi.org/10.1029/2005JC003267>

- Marquet, P. A., Quinones, R. A., Abades, S., Labra, F., Tognelli, M., Arim, M., & Rivadeneira, M. (2005). Scaling and power-laws in ecological systems. *Journal of Experimental Biology*, 208(Pt 9), 1749–1769.
- Menden-Deuer, S., & Lessard, E. J. (2000). Carbon to volume relationships for dinoflagellates, diatoms, and other protist plankton. *Limnology and Oceanography*, 45(3), 569–579.
- Monti, M., Minocci, M., Milani, L., & Umani, S. F. (2012). Seasonal and interannual dynamics of microzooplankton abundances in the Gulf of Trieste (Northern Adriatic Sea, Italy). *Estuarine, Coastal and Shelf Science*, 115, 149–157.
- Mozetič, P., Francé, J., Kogovšek, T., Talaber, I., & Malej, A. (2012). Plankton trends and community changes in a coastal sea (northern Adriatic): Bottom-up vs. top-down control in relation to environmental drivers. *Estuarine, Coastal and Shelf Science*, 115, 138–148.
- Mozetič, P., Solidoro, C., Cossarini, G., Socal, G., Precali, R., Francé, J., Bianchi, F., De Vittor, C., Smolaka, N., & Fonda Umani, S. (2010). Recent trends towards oligotrophication of the northern Adriatic: evidence from chlorophyll a time series. *Estuaries and Coasts*, 33(2), 362–375.
- Naselli-Flores, L., & Barone, R. (2011). Invited review-fight on plankton! Or, phytoplankton shape and size as adaptive tools to get ahead in the struggle for life. *Cryptogamie, Algologie*, 32(2), 157–204.
- Newman, M. E. J. (2005). Power laws, Pareto distributions and Zipf's law. *Contemporary Physics*, 46(5), 323–351.
- Niklas, K. J. (2004). Plant allometry: Is there a grand unifying theory? *Biological Reviews of the Cambridge Philosophical Society*, 79(4), 871–889.
- Nock, C. A., Vogt, R. J., & Beisner, B. E. (2016). *Functional traits* (pp. 1–8). Wiley.
- Oksanen, J., Blanchet, F. G., Friendly, M., Kindt, R., Legendre, P., McGlenn, D., Minchin, P. R., O'Hara, R. B., Simpson, G. L., Solymos, P., Stevens, M. H. H., Szoecs, E., & Wagner, H. (2018). Package 'vegan.' *Community Ecology Package, Version*, 2(9), 1–295.
- Olenina, I., S. Hajdu, L. Edler, A. Andersson, N. Wasmund, S. Busch, J. Göbel, S. Gromisz, S. Huseby, M. Huttunen, A. Jaanus, P. Kokkonen, I. Ledaine and E. Niemkiewicz. (2006). Biovolumes and size-classes of phytoplankton in the Baltic Sea HELCOM. Baltic Sea Environment Proceeding. 106(144).
- Perkins, D. M., Perna, A., Adrian, R., Cermen, P., Gaedke, U., Huete-Ortega, M., White, E. P., & Yvon-Durocher, G. (2019). Energetic equivalence underpins the size structure of tree and phytoplankton communities. *Nature Communications*, 10(1), 255.
- Pugnetti, A., Bazzoni, A. M., Beran, A., BernardiAubry, F., Camatti, E., Celussi, M., Coppola, J., Crevatin, E., Negro, P. D., & Paoli, A. (2008). Changes in biomass structure and trophic status of the plankton communities in a highly dynamic ecosystem (Gulf of Venice, Northern Adriatic Sea). *Marine Ecology*, 29(3), 367–374.
- Reynolds, C. (1980). Phytoplankton assemblages and their periodicity in stratifying lake systems. *Holarctic Ecology*, 3(3), 141–159.
- Roselli, L., Bevilacqua, S., & Terlizzi, A. (2022). Using null models and species traits to optimize phytoplankton monitoring: An application across oceans and ecosystems. *Ecological Indicators*, 138, 108827.
- Roselli, L., & Litchman, E. (2017). Phytoplankton traits, functional groups and community organization. *Journal of Plankton Research*, 39(3), 491–493.
- Ryabov, A., Blasius, B., Hillebrand, H., Olenina, I., & Gross, T. (2022). Estimation of functional diversity and species traits from ecological monitoring data. *Proc Natl Acad Sci U S A*, 119(43), e2118156119.
- Sheldon, R. W., Prakash, A., & Sutcliffe, W. H. (1972). The size distribution of particles in the ocean. *Limnology and Oceanography*, 17(3), 327–340.
- Sieburth, J., Smetacek, V., & Lenz, J. (1978). Pelagic ecosystem structure: Heterotrophic compartments of the plankton and their relationship to plankton size fractions. *Limnology and Oceanography*, 23, 1256–1263.
- Socal, G., I. Buttino, A. Penna, C. Totti, M. Cabrini and O. Mangoni. (2010). Metodologie di studio del Plancton marino.
- Sommer, U., Charalampous, E., Genitsaris, S., & Moustaka-Gouni, M. (2017). Benefits, costs and taxonomic distribution of marine phytoplankton body size. *Journal of Plankton Research*, 39(3), 494–508.
- Sonnet, V., Guidi, L., Mouw, C. B., Puggioni, G., & Ayata, S. D. (2022). Length, width, shape regularity, and chain structure: Time series analysis of phytoplankton morphology from imagery. *Limnology and Oceanography*, 67(8), 1850–1864.
- Sprules, W. G. (1988). Effects of trophic interactions on the shape of pelagic size spectra: With 5 figures in the text. *Internationale Vereinigung Für Theoretische und Angewandte Limnologie: Verhandlungen*, 23(1), 234–240.
- Stanca, E., Cellamare, M., & Basset, A. (2013). Geometric shape as a trait to study phytoplankton distributions in aquatic ecosystems. *Hydrobiologia*, 701(1), 99–116.
- Sun, J., & Liu, D. (2003). Geometric models for calculating cell biovolume and surface area for phytoplankton. *Journal of Plankton Research*, 25(11), 1331–1346.
- Sutton, J. (1997). Gibraltar's legacy. *Journal of Economic Literature*, 35(1), 40–59.
- Svensson, F., Norberg, J., & Snoeijs, P. (2014). Diatom cell size, coloniality and motility: Trade-offs between temperature, salinity and nutrient supply with climate change. *PLoS ONE*, 9(10), e109993.
- Talaber, I., Francé, J., Flander-Putrlle, V., & Mozetič, P. (2018). Primary production and community structure of coastal phytoplankton in the Adriatic Sea: Insights on taxon-specific productivity. *Marine Ecology Progress Series*, 604, 65–81.
- Talaber, I., Francé, J., & Mozetič, P. (2014). How phytoplankton physiology and community structure adjust to physical forcing in a coastal ecosystem (northern Adriatic Sea). *Phycologia*, 53(1), 74–85.
- Totti, C., Romagnoli, T., Accoroni, S., Coluccelli, A., Pellegrini, M., Campanelli, A., Grilli, F., & Marini, M. (2019). Phytoplankton communities in the northwestern Adriatic Sea: Interdecadal variability over a 30-years period (1988–2016) and relationships with meteorological drivers. *Journal of Marine Systems*, 193, 137–153.
- Utermöhl, H. (1958). Vervollkommung der quantitativen phytoplankton-methodik. *Zur Mitteilungen Internationale Vereinigung Für Theoretische und Ange-Wandte Limnologie*, 9, 1–38.
- Vadrucci, M. R., Cabrini, M., & Basset, A. (2007). Biovolume determination of phytoplankton guilds in transitional water ecosystems of Mediterranean Ecoregion. *Transitional Waters Bulletin*, 2, 83–102.
- Varkitzi, I., Francé, J., Basset, A., Cozzoli, F., Stanca, E., Zervoudaki, S., Giannakourou, A., Assimakopoulou, G., Venetsanopoulou, A., Mozetič, P., Tinta, T., Skejic, S., Vidjak, O., Cadiou, J. F., & Pagou, K. (2018). Pelagic habitats in the Mediterranean Sea: A review of good environmental status (GES) determination for plankton components and identification of gaps and priority needs to improve coherence for the MSFD implementation. *Ecological Indicators*, 95, 203–218.
- Vascotto, I., Aubry, F. B., Bastianini, M., Mozetič, P., Finotto, S., & Francé, J. (2024). Exploring the mesoscale connectivity of

- phytoplankton periodic assemblage's succession in northern Adriatic pelagic habitats. *Science of the Total Environment*, 913, 169814.
- Vascotto, I., Mozetič, P., & Francé, J. (2021). Phytoplankton time-series in a LTER site of the Adriatic Sea: Methodological approach to decipher community structure and indicative taxa. *Water*, 13(15), 2045.
- Verdy, A., Follows, M., & Flierl, G. (2009). Optimal phytoplankton cell size in an allometric model. *Marine Ecology Progress Series*, 379, 1–12.
- Weithoff, G., & Gaedke, U. (2016). Mean functional traits of lake phytoplankton reflect seasonal and inter-annual changes in nutrients, climate and herbivory. *Journal of Plankton Research*. <https://doi.org/10.1093/plankt/fbw072>
- Witek, Z., & Krajewska-Soltys, A. (1989). Some examples of the epipelagic plankton size structure in high latitude oceans. *Journal of Plankton Research*, 11(6), 1143–1155.
- Zhang, Q., Cozzi, S., Palinkas, C., & Giani, M. (2020). Recent status and long-term trends in freshwater discharge and nutrient inputs. *Coastal Ecosystems in Transition: A Comparative Analysis of the Northern Adriatic and Chesapeake Bay*. <https://doi.org/10.1002/9781119543626.ch2>